Check for updates

Revisiting the δ Scuti star FG Virginis using *Kepler K2* and *TESS* data

Joyce A. Guzik[1]*, Jason Jackiewicz[2] and Anne M. Hedlund[1,2]

[1]Los Alamos National Laboratory, Los Alamos, NM, United States, [2]Department of Astronomy, New Mexico State University, Las Cruces, NM, United States

FG Virginis is a δ Scuti variable star that was the target of several ground-based multisite photometric campaigns from 1992 to 2004. Over 75 pulsation frequencies were detected (Breger et al., Astron. Astrophys., 2005, 435, 955–965), more than for any other δ Sct star before the era of space photometry. FG Vir was observed for 52 days in 30-minute cadence photometry by the NASA *Kepler* spacecraft *K2* mission in 2016, and for 23 days in 2-minute cadence photometry by the NASA *TESS* spacecraft in 2021. We present light curves and amplitude spectra obtained from these space missions. We find around 30 significant frequencies in the *K2* data, and more than 100 significant frequencies in the *TESS* data. There is good correspondence between the first 10 or so highest-amplitude modes found in the *K2* and *TESS* data and those found from the ground-based multisite campaigns, although the amplitude order is slightly different, indicating some stability in mode frequencies and amplitudes spanning 20 years. However, the 9th highest-amplitude mode of Breger et al. has moved down considerably in amplitude rank, while the 35th highest-amplitude mode has moved up to near the top ten as seen in both the *K2* and *TESS* data. We find several low frequencies between 0.3 and 3 cycles per day in the *TESS* data that were not detected using the ground-based data. If low-frequency pulsations are confirmed, FG Vir would be classified as a δ Sct/γ Dor hybrid variable star. We also review stellar model results and some of the challenges for asteroseismology for this well-studied δ Sct star.

KEYWORDS

stars: pulsations, stars: evolution, asteroseismology, stars: FG Vir, NASA Kepler mission, NASA TESS mission, NASA K2 mission, stars: δ Scuti

1 Introduction

The δ Scuti variables lie at the intersection of the classical Cepheid instability strip with the main sequence (Aerts et al., 2010; Kurtz 2022). They have spectral types A through mid F, effective temperatures 6400–8600 K (Uytterhoeven et al., 2011), and masses 1.4–2.7 $M_\odot$ (Bowman and Kurtz, 2018). Most are in the main-sequence (core hydrogen burning) or slightly post-main-sequence (burning hydrogen in a shell just outside the hydrogen-exhausted core) evolutionary phases, but they have also been found in the pre-main-sequequence phase (see, e.g., Zwintz and Steindl 2022; Murphy et al.,
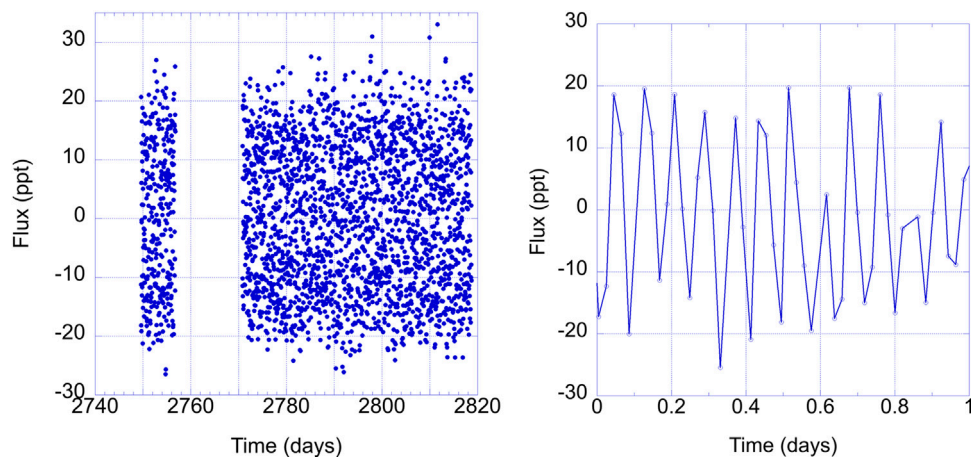
FIGURE 1
Left: FG Vir *K2* 30-min cadence light curve from Campaign 10, showing 52.5 days of data, excluding the gap near the beginning of the data set. Time is measured after barycentric Julian day 2454833.0. Right: Zoom-in on FG Vir *K2* light curve on day 2790.

2021). δ Scuti stars pulsate with frequencies 5–50 c/d (Balona et al., 2015) in one or more radial and non-radial low-order pressure (p) modes, low-order gravity (g) modes, and modes having a mixture of p- and g-type nodes. Their pulsations are driven by the "kappa" opacity-valving effect in the 2nd helium ionization region of the stellar envelope around 50,000 K (Chevalier 1971); in some δ Sct stars the hydrogen ionization region and turbulent pressure may also play a role in pulsation driving (Antoci et al., 2019).

These stars are of interest for asteroseismology, i.e., using the pulsation properties in conjunction with modeling to derive stellar interior structure and to test theories of stellar evolution and pulsation driving (see, e.g., Antoci et al., 2019; Bowman et al., 2021; Daszynska-Daszkiewicz et al., 2021, 2022).

FG Virginis (HD 106384) is a well-studied bright (V = 6.558) δ Scuti star of spectral type A8. FG Vir was the object of ground-based single-site (1982; see Lopez de Coca et al., 1984) and multisite (1992–2004; see Breger et al., 1995, 1996, 1998, 2004, 2005; Breger and Lenz 2019) photometric campaigns. These campaigns resulted in detection of 75+ pulsation frequencies (Breger et al., 2005), more than any other δ Sct star before the era of long time-series space photometric missions such as CoRoT (Poretti et al., 2009), *Kepler* (Borucki et al., 2010; Gilliland et al., 2010; Koch et al., 2010), and *TESS* (Ricker et al., 2015). See also Guzik (2021) and Daszynska-Daszkiewicz et al. (2005, 2021) for more information about δ Sct stars and results from space missions.
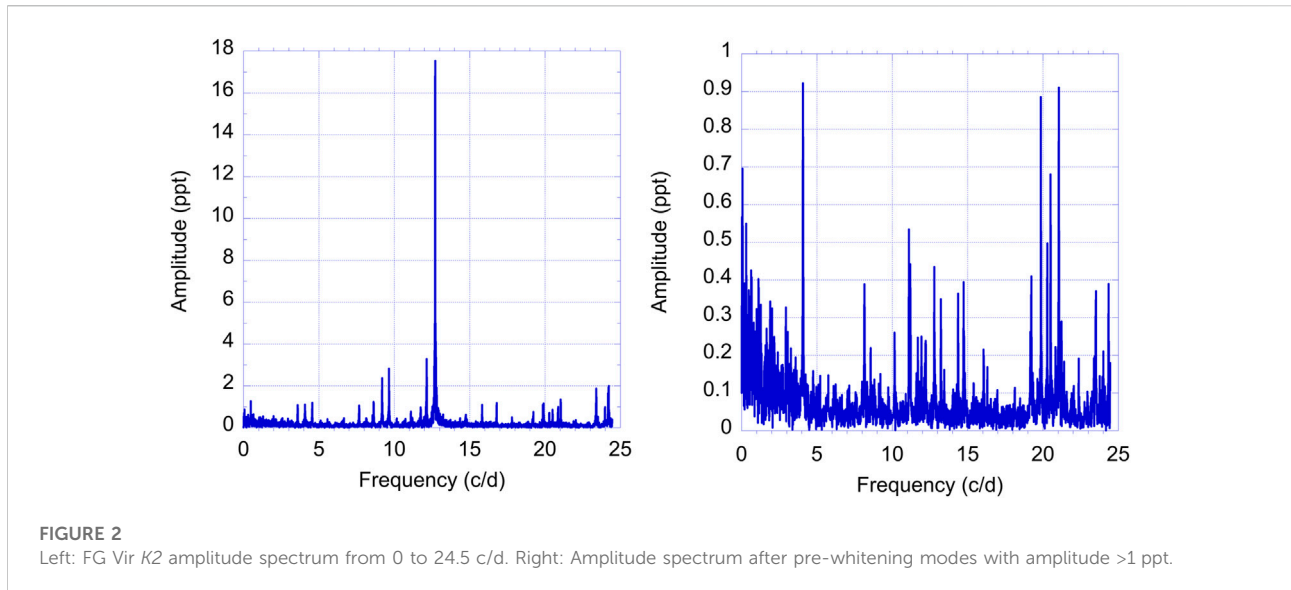
FG Vir was observed for 52.5 days in 30-minute cadence photometry by the NASA *Kepler* spacecraft during Campaign 10 (6 July–20 September 2016) of the extended *Kepler* mission (*K2*, Howell et al., 2014) as part of our request to the Guest Observer program (Guzik et al., 2019). FG Vir was observed by the NASA

TESS spacecraft for 23 days in December 2021. We present a first look at the amplitude spectra derived from these data, and comparisons with the amplitude spectra obtained using the ground-based multisite data. We also review some of the findings from asteroseismology and unanswered questions for this interesting δ Sct star.

2 *Kepler* data analysis and results

FG Vir is EPIC 201132898 in the *K2* Ecliptic Plane Input Catalog (Huber et al., 2016). We retrieved the pre-search data conditioning simple-aperture photometry (PDC_SAP) light-curve data from the Mikulski Archive for Space Telescopes (MAST, https://archive.stsci.edu/), *K2* pipeline data release 37, January 2020. Figure 1 shows the *K2* light curve and a 1-day zoom-in on a portion of the light curve. Figure 2 shows the amplitude spectrum resulting from a Fourier analysis of the light curve and the amplitude spectrum after pre-whitening all frequencies with amplitude >1 ppt. To determine the significant frequencies, the highest-amplitude modes were removed from the light curve successively until only noise remained, a process called pre-whitening. For evenly spaced 29.4244-min cadence data, the Nyquist frequency limit is 24.4695 c/d, so the amplitude spectrum is truncated at this frequency. In reality, the *K2* data are not exactly evenly spaced because of light travel-time corrections due to the spacecraft's orbit around the solar system barycenter (Murphy et al., 2013).

Table 1 lists the 34 frequencies obtained from the pre-whitening analysis in order of signal-to-noise (S/N) ratio, down to S/N = 4.0. Uncertainties on frequencies and amplitudes were calculated using the process derived by

FIGURE 2
Left: FG Vir *K2* amplitude spectrum from 0 to 24.5 c/d. Right: Amplitude spectrum after pre-whitening modes with amplitude >1 ppt.

Montgomery and O'Donoghue (1999). Table 1 also notes associations of these frequencies with those from Breger et al. (2005) obtained using multisite observations. Considering the first 9 modes, all of them are found among the 10 highest-amplitude modes of Breger et al., although the amplitude ordering is slightly different. Breger et al.'s 9th highest-amplitude mode (frequency 19.228 c/d) is only the 14th highest-amplitude using the *K2* data. Many of the remaining frequencies found in the *K2* data can be associated with the Breger et al. frequencies. It is interesting that the 35th highest-amplitude mode in the Breger et al. list (frequency 20.511 c/d) corresponds to the 11th highest in the *K2* data. While Breger et al. (2005) adopted a S/N limit of 4 for a significant detection, this limit may be too low for space-based data (Baran and Koen 2021; Bowman and Michielsen 2021) and so the list may contain some false detections. However, we find frequencies in the *K2* data associated with Breger et al. (2005) frequencies down to a S/N of 4 and lower. Frequencies at 11.69952 and 11.94247 c/d were also found in the *K2* data, corresponding to f33 and f29, respectively, in the Breger et al. list, but these modes have S/N ratio 3.27 and 3.14, respectively, in the *K2* analysis, and were not included in the table.

To compensate for the loss of a second reaction wheel, the *K2* mission used solar radiation pressure to keep the spacecraft pointed in the same direction, and in addition fired thrusters every 5.8849 h (*K2* Handbook, Mighell and Van Cleve 2020). The thruster-firing frequency of 4.0782 c/d and its harmonic at 8.1564 c/d appear in the *K2* frequency list.

We searched for combination frequencies by algorithm with tolerance of 10% of the inverse of the time series length. For the *K2* data with length 69.121 days, the tolerance is 0.001446 c/d. We found no combination frequencies among the list in Table 1.

Table 1 lists nine modes with frequencies 0.3 to ~3 c/d, in the right frequency range to be γ Dor gravity modes (see, e.g., Aerts et al., 2010; Li et al., 2020). Six of these are among the lowest-amplitude modes, with S/N < 4.5, and are likely to be spurious. However, if low-frequency modes were to be detected, FG Vir would be considered a hybrid δ Sct/γ Dor variable-star candidate.

The multisite data is not evenly spaced, so the 24.4695 c/d *K2* Nyquist limit does not apply, and Breger et al. (2005) find frequencies up to 44.2591 c/d. One *K2* frequency at 14.36915 c/d was found that could be a Nyquist reflection of the 34.5737 f23 mode of the Breger et al. list. We also made use of the *TESS* data with higher Nyquist limit (see below) to verify that only this one frequency in the *K2* list is a Nyquist alias.

3 *TESS* data

The *Kepler* spacecraft was retired in November 2018; the *TESS* spacecraft (Ricker et al., 2015) was launched in April 2018 into a 13.7-day elliptical orbit around Earth, maintained by a 2:1 lunar resonance. *TESS* data for FG Vir is now available at MAST, taken during the 27.4 observing days of sector 46 (December 2–30, 2021). Moreover, data were taken at 2-minute cadence, so the S/N is much larger, and the Nyquist frequency limit is 360 c/d, much higher than for 30-min cadence *K2* data.

FG Vir is TIC 277227048 in the *TESS* Input Catalog (Stassun et al., 2019). Figure 3 (left) shows the *TESS* FG Vir light curve, including data from 22.84 days, excluding the gap of about 5 days in the middle of the data set. Figure 3 (right) shows a 1-day zoom-in on the light curve; small features are resolved in the *TESS* 2-min cadence light curve that were not resolvable in *K2* 30-min cadence light curve.

TABLE 1. FG Vir *K2* frequencies in order of S/N compared with Breger et al. (2005) frequencies. Low frequencies between 0.3 and ~3 c/d are highlighted using red font. The calculated uncertainties in *K2* frequencies and amplitudes, respectively, are 4.22×10⁻⁴ c/d and 50.1 ppm.

Freq. #	Freq. (c/d)	Amplitude (ppt)	S/N	Notes	Breger et al. freq. (c/d)	Breger et al. freq. #	Breger et al. S/N
f1	12.71617	15.943	171.48		12.7162	f1	442
f2	12.15361	2.805	30.19		12.1541	f2	85
f3	9.65608	2.667	28.90		9.6563	f5	71
f4	9.19909	2.062	22.16		9.1991	f7	53
f5	24.22769	1.868	19.54		24.2280	f3	74
f6	23.40337	1.676	17.95		23.4034	f4	71
f7	24.19443	1.441	15.34		24.1940	f10	29
f8	21.05045	1.188	12.50		21.0515	f6	55
f9	19.86748	0.959	10.26		19.8679	f8	55
f10	4.07820	0.775	9.96	*K2* thruster frequency			
f11	20.51103	0.815	8.52		20.5112	f35	6.6
f12	20.28543	0.630	7.00		20.2878	f11	26
f13	0.31527	0.593	6.53	Low frequency			
f14	19.22828	0.575	6.16		19.2278	f9	30
f15	11.10514	0.557	5.93		11.1034	f20	11
f16	4.09555	0.525	5.79				
f17	0.63921	0.474	5.64	Low frequency			
f18	0.52930	0.538	5.50	Low frequency			
f19	12.79427	0.492	5.28		12.7944	f17	13
f20	14.36915	0.479	4.94	Nyquist reflection	34.5737[a]	f23	9.3
f21	11.21071	0.479	4.88		11.2098	f38	6.4
f22	23.50894	0.442	4.76				
f23	13.23679	0.414	4.53		13.2365	f27	8.3
f24	14.73503	0.412	4.46		14.7354	f49	5.3
f25	1.91184	0.373	4.38	Low frequency			
f26	0.67536	0.411	4.34	Low frequency			
f27	8.15785	0.402	4.31	2x *K2* thruster frequency			
f28	1.29143	0.411	4.30	Low frequency			
f29	1.12657	0.406	4.25	Low frequency			
f30	24.34917	0.384	4.23		24.3485	f18	12
f31	0.49314	0.421	4.13	Low frequency			
f32	4.06518	0.386	4.07				
f33	21.23122	0.371	4.04		21.2323	f16	14
f34	0.47434	0.371	4.03	Low frequency			

[a]Frequency reflected around Nyquist frequency of 24.4695 c/d.

Figure 4 shows the FG Vir amplitude spectrum using *TESS* data, truncated at 50 c/d, and the amplitude spectrum after pre-whitening frequencies with amplitude >1 ppt. Figure 5 shows the K2 and TESS amplitude spectra overlayed. Table 2 lists the first 100 frequencies pre-whitened in order of amplitude, and notes associations with Breger et al. (2005) frequencies. Uncertainties on frequencies and amplitudes were determined using the process derived by Montgomery and O'Donoghue (1999). The highest frequency on this list is 42.1 c/d. The 9 highest-amplitude *TESS* frequencies are among the 10 highest-amplitude Breger et al. (2005) frequencies, although the amplitude order is slightly different. The 9th highest-amplitude frequency in the Breger et al. list is 28th highest in the *TESS* list, while f35 in the Breger et al. list is 11th highest in the *TESS* list, confirming the significant amplitude changes in these modes found using the *K2* data.

The S/N ratio of the 100th frequency in the list is 31, so it is likely that many more significant frequencies remain in the residual. Continued pre-whitening results in 718 additional frequencies with S/N ratio >4. However, we hesitate to claim that all of these frequencies are separate intrinsic frequencies. Handler (2009) points out several reasons why spurious small-amplitude peaks may be found in pre-whitening analyses. These
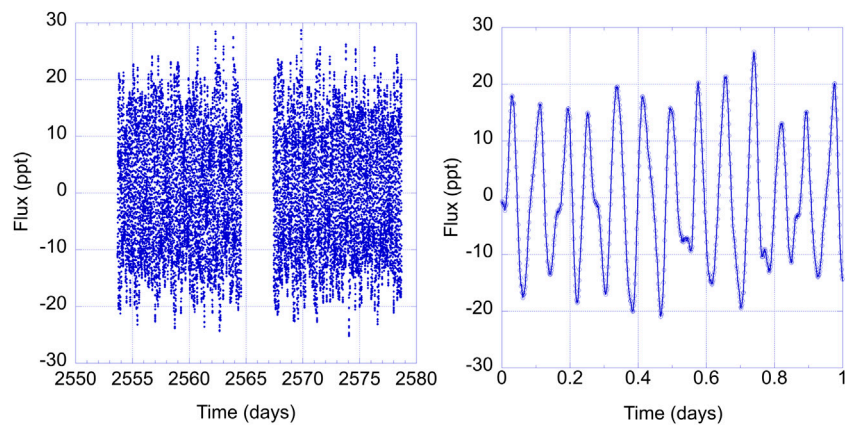
FIGURE 3
Left: FG Vir *TESS* 2-min cadence light curve from sector 46, showing 22.84 days of data, excluding the ~5-day gap in the middle of the data set. Time is measured after barycentric Julian day 2457000. Right: Zoom-in on *TESS* light curve on day 2560. Small features are resolved that were not resolved using *K2* 30-min cadence data.
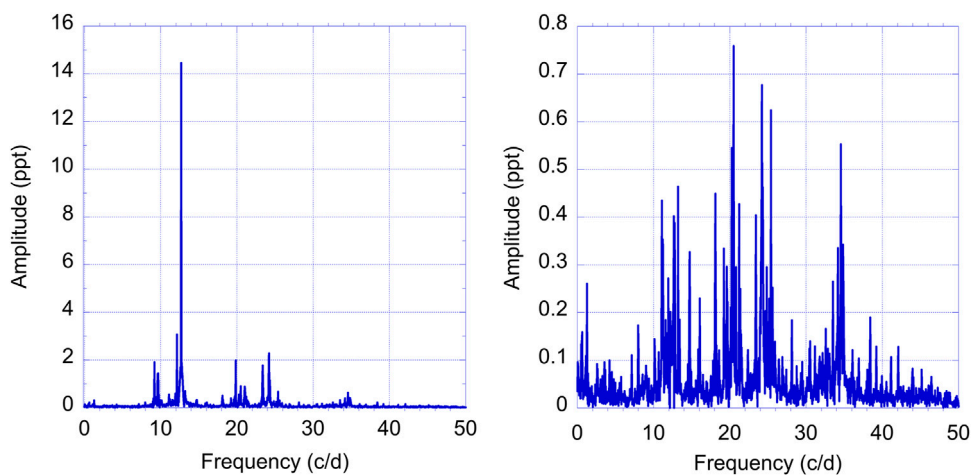

FIGURE 4
Left: FG Vir amplitude spectrum from *TESS* 2-min cadence data. Right: Amplitude spectrum after pre-whitening modes with amplitude >1 ppt.

reasons include short time-series limit, non-sinusoidal light curve shape, amplitude and frequency variations, and modulation from stellar or substellar companions.

Table 2 includes five low frequencies between 0.3 and ~3 c/d, highlighted in red font. These frequencies are more likely to be real, as opposed to the low frequencies in the *K2* data, as their S/N ratio is high. These low frequencies do not coincide with any of the likely spurious low frequencies found in the *K2* data. If confirmed as gravity-mode pulsations, FG Vir would be classified as a δ Sct/γ Dor hybrid. To confirm these frequencies would require ruling out spacecraft artifacts, light curve contamination by nearby or background objects, and rotation (possibly

differential) and starspots as the source of the low frequencies. Time-series spectroscopy may be useful, e.g., to distinguish starspots, which may show signatures of chromospheric activity, or to detect line-profile variations on the expected timescales, indicating nonradial pulsations. Perhaps it may be possible to directly image starspots on FG Vir using optical interferometry (see, e.g., Cunha et al., 2007).

We searched for combination frequencies by algorithm with tolerance of 10% of the inverse of the time-series length. For the *TESS* data set with length 25.008 days, this tolerance is 0.003998 c/d. Because of this high tolerance, many combinations were found; however, many of these
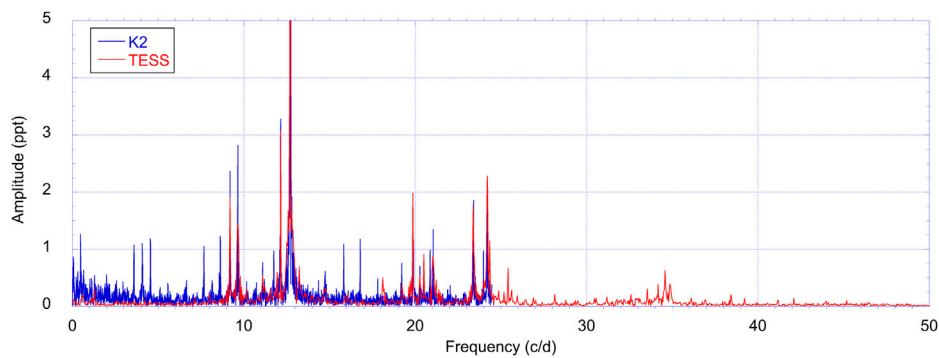
FIGURE 5
FG Vir *K2* and *TESS* amplitude spectra overlayed. The amplitude axis has been truncated at 5 ppt to show the low-amplitude peaks.

combinations involve lower-amplitude modes, and are likely to be fortuitous (see also discussions by Papics 2012; Kurtz et al., 2015). A longer series of *TESS* data would help to sort out intrinsic from combination frequencies.

The *Kepler/K2* photometry has a bandpass of 400–850 nm, while the *TESS* bandpass is redder, 600–1000 nm. Because of FG Vir's late-A spectral type, its mode amplitudes are therefore generally higher using the *K2* data compared to the TESS data. Although the *K2* and *TESS* data time series discussed in this paper are relatively short and non-overlapping, it is possible that phase differences between modes using photometric time-series data taken at different bandpasses could be exploited for mode identification in the same way that techniques using multi-color ground-based data were applied for FG Vir mode identification.

4 Unresolved questions for asteroseismology

As discussed by, e.g., Guzik (2021), there are many inter-related unresolved problems for δ Sct stars that make asteroseismology challenging.

First, there is a mode visibility problem for non-radial oscillations as seen in δ Sct stars. Temperature variations described by spherical harmonic patterns average out over the unresolved stellar disk, making higher degree (ℓ) modes more difficult to see in photometry. Usually, it is expected to detect modes of degree 0 (radial), 1 (dipole), and 2 (quadrupole). Is it possible to measure modes of degree $\ell = 3$ or higher, particularly with the higher precision and longer continuous time series of space-based photometry? Daszynska-Daszkiewicz et al. (2006) conclude that modes of degree $\ell = 3$ and probably much larger ℓ should be visible, even using the FG Vir ground-based data, and that most of the modes discovered for FG Vir below 30 c/d must have $\ell > 2$.

Second is the rotational splitting problem. Stellar rotation splits modes into a multiplet of $2\ell + 1$ frequencies. Rotation also shifts frequencies so that the multiplet members are not equally spaced (Goupil and Dziembowski 2000). Rotation can shift frequencies even for radial ($\ell = 0$) modes (see, e.g., Di Criscienzo et al., 2008) and the $m = 0$ multiplet of non-radial modes (Saio 1981). Rotation also makes a star oblate and changes its mean density, affecting the accuracy of radial mode frequencies predicted using non-rotating models (Murphy et al., 2022). FG Vir's equatorial rotation velocity is 30–80 km/sec (Mantegazza and Poretti 2002; Zima et al., 2006), so we should expect a rotational splitting frequency of around 0.5 c/d for FG Vir stellar radius ~2.2 $R_\odot$. We do not see obvious rotationally split modes in the FG Vir amplitude spectrum.

Third is the mode selection problem. Not all of the modes expected from stellar models for δ Sct stars are seen in the amplitude spectrum (see, e.g., Bedding et al., 2020; Murphy et al., 2021). Also, there are modes observed that are not expected from the best-fit pulsation models.

Then there is the mystery of amplitude and frequency variations found in many types of variable stars including δ Sct stars (see, e.g., Bowman et al., 2016). Amplitudes and frequencies of individual δ Sct modes can be relatively stable over time. It is possible to associate many of the highest-amplitude frequencies in the *K2* (2016) and *TESS* (2021) data sets with frequencies in the Breger et al. (2005) list. However, the order of the mode amplitudes is somewhat different for the first dozen or more modes; some modes appear in the *K2* and *TESS* data that are not in the Breger et al. list, and vice versa; and the Breger et al. f9 mode has moved down in amplitude rank, while the f35 mode increased in rank. Nonlinear mode-coupling effects (see, e.g., Buchler and Regev 1983; Buchler et al., 1997; Dziembowski 1993) are suspected as the cause of these variations.

TABLE 2. 100 highest S/N FG Vir *TESS* frequencies. Low frequencies between 0.3 and ~3 c/d are highlighted using red font. The calculated uncertainties in *TESS* frequencies and amplitudes, respectively, are 3.79×10⁻⁴ c/d and 9.82 ppm.

Freq. #	Freq. (c/d)	Amplitude (ppt)	S/N	Potential combinations and notes	Breger et al. freq. #
f1	12.7151	13.671	3776.72	—	f1
f2	24.2107	2.663	811.51	—	f3
f3	12.1553	2.468	702.20	—	f2
f4	9.6563	2.295	641.36	—	f5
f5	23.4070	2.029	577.76	—	f4
f6	19.8684	1.961	528.05	—	f8
f7	9.2005	1.793	498.21	—	f7
f8	21.0519	1.369	365.23	—	f6
f9	24.2427	0.996	253.82	—	
f10	24.1747	0.857	227.61	2f9-2f3	
f11	20.5121	0.795	226.58	—	f35
f12	34.5708	0.769	208.61	—	f23
f13	20.2882	0.756	204.74	—	f11
f14	25.4343	0.679	191.88	—	f15 = 2f1
f15	12.6871	0.580	182.56	—	
f16	18.1291	0.611	170.30	—	
f17	34.8826	0.570	168.79	—	
f18	11.0998	0.537	158.94	—	f20
f19	24.3547	0.557	150.51	—	
f20	11.2117	0.535	149.78	—	f38
f21	14.7344	0.534	148.38	3f8-2f2	f49
f22	13.2389	0.484	139.21	—	f27
f23	23.4350	0.363	133.53	—	f24
f24	21.2319	0.439	127.39	—	f16
f25	19.6445	0.414	116.93	—	f65
f26	12.7951	0.411	114.59	—	f17
f27	34.1949	0.393	105.00	—	f54?
f28	19.2286	0.361	101.11	—	f9
f29	11.9434	0.345	92.45	—	f29
f30	20.8320	0.329	91.89	—	f39
f31	33.5352	0.328	90.38	—	
f32	1.2875	0.310	87.64	2f11-2f6, low frequency	
f33	24.8705	0.267	76.71	1f3+1f1	f36 = f1+f2
f34	25.6342	0.273	73.29	3f24-3f15	f68
f35	23.4870	0.251	69.59	2f37-2f4	
f36	12.6072	0.199	69.52	—	
f37	16.0738	0.259	69.43	2f30-2f26	f13
f38	21.3998	0.257	68.96	1f27-1f26	f46
f39	25.1824	0.240	67.81	1f29+1f22	
f40	24.1428	0.288	67.40	—	
f41	19.3246	0.235	64.74	—	f41
f42	12.7511	0.230	64.23	—	
f43	12.1274	0.227	63.85	—	
f44	38.4173	0.220	61.63	1f16+1f13	
f45	28.1412	0.222	61.30	—	f19?
f46	11.6076	0.233	60.52	2f13-3f4	f50

(Continued on following page)

TABLE 2. (*Continued*) 100 highest S/N FG Vir *TESS* frequencies. Low frequencies between 0.3 and ~3 c/d are highlighted using red font. The calculated uncertainties in *TESS* frequencies and amplitudes, respectively, are 3.79×10^{-4} c/d and 9.82 ppm.

Freq. #	Freq. (c/d)	Amplitude (ppt)	S/N	Potential combinations and notes	Breger et al. freq. #
f47	13.4469	0.216	59.77	—	
f48	0.5038	0.210	58.49	2f41-3f1, low frequency	
f49	23.9988	0.216	58.14	—	f58
f50	23.3750	0.208	56.87	—	
f51	7.9889	0.199	56.34	—	f44
f52	34.1189	0.194	55.22	—	f72
f53	10.1721	0.190	54.33	—	f25
f54	24.5426	0.173	51.91	—	
f55	34.7627	0.183	51.33	—	
f56	22.3714	0.176	50.03	1f4+1f1	f42 = f1+f5
f57	12.2313	0.180	49.32	2f32+1f4	
f58	32.5835	0.171	49.03	1f6+1f1	
f59	21.4678	0.166	46.60	—	
f60	18.1650	0.161	46.23	—	
f61	31.2000	0.163	45.60	—	f57
f62	36.1182	0.163	44.93	1f29+1f10	f40 = f1+f4
f63	21.5677	0.155	43.91	2f38-1f24	
f64	33.9990	0.155	43.56	2f50-1f42	
f65	11.7875	0.180	43.42	—	
f66	30.4563	0.159	42.92	—	
f67	0.5918	0.152	41.92	1f49-1f5, low frequency	
f68	39.2170	0.151	41.37	—	f69
f69	11.7115	0.156	41.15	—	
f70	30.5483	0.147	40.86	—	
f71	2.6590	0.143	40.19	Low frequency	
f72	20.0643	0.144	40.18	2f13-1f11	
f73	34.6547	0.145	39.38	—	
f74	20.6681	0.138	39.37	—	
f75	32.1797	0.137	39.27	—	
f76	32.8554	0.143	39.14	—	
f77	11.4876	0.134	38.22	—	f70? = f3-f1
f78	31.7718	0.137	38.00	1f43+1f25	
f79	23.8069	0.134	37.63	2f32+1f24	f48
f80	42.1039	0.133	37.30	2f8	f64 = 2f6
f81	15.8659	0.141	37.02	—	
f82	18.6009	0.135	36.95	—	
f83	14.5424	0.132	36.81	—	
f84	26.9217	0.130	36.41	1f34+1f32	f61?
f85	33.0433	0.131	36.35	—	f74
f86	25.9421	0.124	36.04	—	
f87	24.6666	0.126	34.99	—	
f88	25.3863	0.124	34.32	2f33-1f19	
f89	7.1493	0.121	34.31	3f23-3f8	
f90	41.1922	0.123	34.23	—	
f91	17.8212	0.122	33.98	—	

(Continued on following page)

TABLE 2. (*Continued*) 100 highest S/N FG Vir *TESS* frequencies. Low frequencies between 0.3 and ~3 c/d are highlighted using red font. The calculated uncertainties in *TESS* frequencies and amplitudes, respectively, are 3.79×10^{-4} c/d and 9.82 ppm.

Freq. #	Freq. (c/d)	Amplitude (ppt)	S/N	Potential combinations and notes	Breger et al. freq. #
f92	29.4927	0.122	33.90	—	
f93	16.1058	0.121	33.44	2f33-3f20	f31
f94	11.1317	0.121	33.43	2f14-2f6	
f95	8.8966	0.120	33.01	1f8-1f3	
f96	10.6839	0.121	32.85	—	f79 = f4-f1
f97	3.0588	0.118	32.61	Low frequency	
f98	26.5298	0.115	32.39	—	f71
f99	8.5767	0.117	32.34	—	
f100	4.2424	0.113	31.34	2f29-1f25	

Breger and Pamyatnykh (2006) investigate the problem of closely spaced modes in FG Vir, with separations less than 0.1 c/d, too small to be the result of rotational splitting. Are these separate modes, or are they the result of amplitude variability of a single frequency? Breger and Pamyatnykh (2006) were able to rule out amplitude variability for several of the FG Vir closely spaced modes.

These many complications lead to a mode identification problem. We cannot identify modes by patterns in the amplitude spectrum and match them directly with modes expected from theoretical models. However, methods have been developed to identify the angular degree (ℓ) and azimuthal order (m) of the highest-amplitude modes using multi-color photometry, phase information, line profile variations and radial velocities from spectroscopy (see, e.g., Viskum et al., 1998; Breger et al., 1999, Mantegazza and Poretti 2002, Daszynska-Daszkiewicz et al., 2005; Zima et al., 2006). Some FG Vir modes have been identified using these methods, but mode identification has been somewhat uncertain. For example, Daszynska-Daszkiewicz et al. (2005) identified the angular degrees for twelve FG Vir modes to 80% probability, but there are ambiguities for six of these modes. In early studies of FG Vir, the highest-amplitude mode at 12.7162 c/d was thought to be the radial fundamental mode (e.g., Mantegazza et al., 1994; Breger et al., 1995), but later studies (e.g., Viskum et al., 1998; Mantegazza and Poretti 2002) showed that this mode is most likely an $\ell = 1$ dipole mode, and the radial fundamental mode actually is the 2nd-highest-amplitude mode at 12.1541 c/d.

Attempts have been successful to find patterns of frequency spacings in δ Sct stars (e.g., Breger et al., 2009). The spacings could correspond to the large separations between modes of successive ℓ values, or a rotational splitting spacing, or a combination of these two spacings (see also Paparo et al., 2016a; Paparo et al., 2016b; Suarez et al., 2014; Bedding et al., 2020). Bedding et al. (2020) found very regular patterns of high-frequency modes in a sample of young δ Sct stars observed by

TESS and *Kepler*, enabling definitive mode identification. Patterns of mode spacings can therefore be useful to identify modes of common ℓ value, determine the stellar mean density, or even to measure the stellar interior rotation rate.

5 FG Vir models

The goal of asteroseismology of FG Vir is to use the observed frequency properties to determine the stellar interior structure and evolution state. Evolution and pulsation models of FG Vir have been calculated over the years to attempt to make use of the observed frequencies. It is helpful to have additional constraints from multi-color photometry, spectroscopy, and stellar model grids to provide a starting point for detailed model explorations. The *TESS* Input Catalog (TIC, Stassun et al., 2019) lists FG Vir properties derived from several sources and methods: effective temperature T_{eff} = 7361 ± 131 K, log surface gravity (log g) = 3.974 ± 0.086, radius R = 2.205 ± 0.082 $R_\odot$, mass M = 1.6 ± 0.282 $M_\odot$, luminosity L = 12.86 ± 0.44 $L_\odot$, and distance 83.02 ± 0.37 pc.

Viskum et al. (1998) use models and frequencies scaled from a 2.2 $M_\odot$ non-rotating evolution model of Christensen-Dalsgaard (1993) to derive a mean stellar density (ρ) = 0.1645 ± 0.005 $\rho_\odot$ for FG Vir. Assuming T_{eff} = 7500 K and metallicity Z = 0.02, they find M = 1.82 ± 0.03 $M_\odot$, L = 14.1 ± 0.9 $L_\odot$, R = 2.227 ± 0.012 $R_\odot$, and log g = 4.002 ± 0.003. Their derived luminosity places FG Vir at a distance of 82 ± 3 pc.

Breger et al. (1999) find a best-fit model to the FG Vir frequencies with M = 1.95 $M_\odot$, T_{eff} = 7492 K, L = 14.92 $L_\odot$, R = 2.301 $R_\odot$, and log g = 4.002. This model has metallicity Z = 0.02, initial helium mass fraction Y = 0.28, and mean density 0.1597 $\rho_\odot$. The model uses artificially modified opacities, has mixing-length parameter α = 1.0, and included core convective overshooting with overshooting distance 0.2 pressure scale heights. The models were evolved without rotation, but

TABLE 3 Unstable low-degree frequencies of 1.82 M$_\odot$ FG Vir model.

Mode degree	Freq. (c/d)	Linear growth rate per period	Notes
0	12.1557	2.87E-06	Radial fundamental mode
0	15.7240	3.30E-05	
0	19.4744	1.66E-04	
0	23.2361	5.67E-04	
0	27.0256	1.54E-03	
0	30.8235	3.32E-03	
0	34.6365	4.67E-03	
0	38.5319	3.27E-03	
1	9.4303	5.92E-09	
1	12.4568	3.87E-06	Nearest frequency to highest-amplitude observed mode
1	16.1672	4.23E-05	
1	19.6468	9.23E-05	
1	20.7309	1.61E-04	
1	24.3940	8.35E-04	
1	28.4415	2.24E-03	
1	32.3942	4.19E-03	
1	36.3191	4.57E-03	
1	40.3270	1.55E-03	
2	10.0989	5.41E-08	
2	11.8952	6.09E-07	
2	12.5352	1.72E-06	
2	14.3243	8.09E-06	
2	16.7172	3.68E-05	
2	19.3467	1.17E-04	
2	22.5367	4.33E-04	
2	26.3052	1.32E-03	
2	30.2200	3.06E-03	
2	32.6560	2.60E-04	
2	34.2273	4.55E-03	
2	38.1374	3.61E-03	
3	8.8390	4.69E-09	
3	9.7564	2.42E-09	
3	10.5646	1.52E-07	
3	11.9282	1.25E-06	
3	13.9073	3.88E-06	
3	15.5789	2.23E-05	
3	16.8010	2.97E-06	
3	18.7368	7.41E-05	
3	20.2535	1.23E-04	
3	23.6239	6.51E-04	
3	27.6333	1.87E-03	
3	31.6207	3.86E-03	
3	35.5724	4.76E-03	
3	39.4859	1.51E-03	
3	39.7631	8.63E-04	

rotational splitting was taken into account up to second order in the pulsation frequency comparisons. The best-fit model had rotation velocity 32 km/sec.

Templeton et al. (2001) find a best-fit model for FG Vir with $M = 1.9 M_\odot$, $T_{eff} = 7413$ K, $L = 14.16 L_\odot$, and age 0.93 Gyr. This model has $Z = 0.03$ and hydrogen mass fraction $Y = 0.28$. The model was evolved without rotation, used mixing-length parameter $\alpha = 1.92$, and includes core convective overshooting with overshooting distance 0.3 pressure scale heights. First-order rotational splitting was taken into account in the pulsation frequency comparisons, assuming rotation velocity 50 km/sec.

Kirbiyik et al. (2004) evolve models with uniform rotation and conservation of angular momentum, and calculate pulsation frequencies including first-order rotational splitting. Their paper does not discuss whether convective overshooting is included. They find best-fit models for FG Vir with $M = 1.85 M_\odot$, $T_{eff} = 7540$–7560 K, $L = 15.06$–$15.12 L_\odot$ and rotation rate 32–66 km/s.

Table 3 lists the $\ell = 0$, 1, 2, and 3 pulsationally unstable frequencies (positive linear growth rates) for an FG Vir model calculated by Guzik. The frequencies include p modes, modes with mixed p-mode and g-mode character, and a few low-order g modes which have frequencies lower than the radial fundamental mode. These model frequencies were used by Paparo et al. (2016a), Paparo et al. (2016b) to illustrate how frequency spacings could be used to help identify modes in δ Scuti stars. The physics of the models is the same as used in the Guzik et al. (2000) FG Vir models, except for minor opacity table updates. The evolution models have mixing-length parameter $\alpha = 1.77$, and do not include rotation or core convective overshooting. A model was selected on the 1.82 $M_\odot$, $Z = 0.02$, $Y = 0.28$ evolutionary track that has radial fundamental mode frequency near 12.1541 c/d, identified as the FG Vir radial fundamental mode. For this model, $L = 13.92 L_\odot$, $T_{eff} = 7419$ K, $R = 2.26 R_\odot$, log g = 3.9896, and mean density 0.1577 $\rho_\odot$. The model age is 0.867 Gyr, and core helium mass fraction is 0.708, indicating that about 2/3 of the core hydrogen has been converted to helium.

The calculated model frequencies in Table 3 do not include rotational splitting, which will divide non-radial modes multiplets with $2\ell + 1$ components, with spacings of around 0.5 c/d, depending on the rotational velocity adopted. Rotation will cause the multiplet members to be unequally spaced in frequency. A total of 98 $\ell = 0$, 1, and 2 modes are predicted, taking into account rotational splitting. However, even including rotational splitting, not all of the observed frequencies of Breger et al. (2005) can be matched for FG Vir. Considering in addition the 15 calculated unstable $\ell = 3$ modes would increase the total number of predicted modes by another 105, to 203. These predictions assume that FG Vir has an inclination such that all modes of a multiplet are visible. As discussed in Section 4, it is possible that modes of even higher angular degree are visible in photometric data.

Breger and Pamyatnykh (2006) found 18 frequency doublets with frequency spacing < 0.1 c/d in their FG Vir frequency list. They

concluded that accidental agreement between frequencies of excited modes can be ruled out because of the large number of doublets. We examined our $\ell = 0$–3 frequency list in Table 3 for close frequency spacings. Only three pairs with spacing <0.1 c/d are found if rotational splitting is not taken into account. However, assuming the nonradial modes are split into $2\ell + 1$ multiplets with 0.5 c/d spacing between multiplets, we find 88 close frequency pairs. While this assumption of equally spaced multiplets is not realistic, this example does show that accidental agreements could explain the close spacings if modes of high-enough degree are visible.

We do not include in Table 3 high-order g-mode frequencies. These frequencies are predicted to have negative growth rates in our pulsation analyses because the envelope convection zone is too shallow (temperature at the base 54,000 K) to drive γ Doradus-type gravity modes via the convective blocking mechanism (Guzik et al., 2000). Nevertheless, many δ Sct stars show low-frequency modes in the γ Dor frequency range (Grigahcene et al., 2010; Uytterhoeven et al., 2011; Balona 2014).

The stellar properties derived for FG Vir using asteroseismic data and stellar models are in good agreement with each other. However, none of the models provided an exact fit to all of the observed FG Vir frequencies, and there is much more that could be learned about FG Vir's evolution and interior structure using ground-based data as well as the *K2* and *TESS* data.

The models available in the literature are quite old, having been calculated in 2004 or earlier, before Gaia parallaxes and revised lower solar abundance determinations (e.g., Asplund et al., 2021). FG Vir should be revisited taking into account modern constraints and using updated modeling tools, for example, using the MESA evolution code (see Paxton et al., 2019 and references therein).

It is an interesting question whether FG Vir has a stellar or planetary companion, and whether these objects might affect pulsation properties. FG Vir is listed as a visual binary in the catalog of Liakos and Niarchos (2017), who reference catalogs of Abt (1981) and Mason et al. (2001). However, the properties of the binary companion and orbital period are not given in these catalogs. An angular separation of 0.1 arc sec is given by Mason et al. (2001), but this separation may be a lower limit to the resolution of the observations.

Kervella et al. (2019) use Hipparcos (van Leeuwen 2007) and Gaia Early Data Release 3 (Gaia Collaboration 2016; Gaia Collaboration 2020; Brown et al., 2021a; 2021b) data to discover stellar and substellar companions using proper motion anomalies. For FG Vir they find no low velocity resolved companions, no bound resolved companions, and no common proper motion candidate companions. They find a tangential velocity anomaly of 6.89 m/s with position angle 196.22 deg. Using their assumptions for a potential orbit and assuming FG Vir mass $M_1 = 1.85 M_\odot$, they derive a companion mass $M_2 = 2.10 M_{Jup}$ (3 AU orbit), 1.05 M_{Jup} (5 AU orbit), or 1.31 M_{Jup} (10 AU orbit). Therefore, we conclude that FG Vir does not have a stellar companion that could affect the analysis, but it may have a substellar one.

6 Conclusion

We compare the FG Vir frequencies detected using 52.4 days of 30-min cadence *Kepler K2* photometry with those detected using at least 363 nights (Breger and Lenz 2019) of multisite ground-based network data. More than 75 significant frequencies were measured in the ground-based data (Breger et al., 2005), compared to around 30, depending on S/N limit adopted, using the *K2* data. The *K2* frequency detections were limited to frequencies below the Nyquist frequency limit of ~24.5 c/d for 29.4-min cadence nearly equally spaced data, while frequencies as high as 44.25 c/d were identified using the ground-based data. The ground-based multisite data included multi-color photometry, which turned out to be extremely useful for mode identifications of the highest-amplitude modes.

The *TESS* data appear more promising for further FG Vir discoveries. The time-series length of the *TESS* data was 22.84 days, shorter than for the *K2* series, but the shorter 2-minute cadence increased greatly the S/N, allowing the detection of at least 100 modes with S/N > 31. The 2-minute cadence also increased the Nyquist frequency limit, so that modes up to 45 c/d, as found in the ground-based data, were detected. The *TESS* data should reveal many more modes of even lower amplitude than found in the ground-based data, requiring consideration of modes of angular degree $\ell > 3$ for asteroseismic models. The increased number of detected modes will make mode identification even more challenging.

There is general agreement among the frequencies of the 10 or so highest-amplitude modes between the ground-based, *K2*, and *TESS* data. Two modes of interest are the f9 mode of Breger et al. (2005), which moved down in amplitude rank, and the f35 mode of Breger et al., which moved up in amplitude rank according to both the *K2* and *TESS* data.

The continuity of the *K2* and *TESS* time-series data, and, possibly, the elimination of day/night aliases, enables detection of low-frequency modes. Several modes of significant amplitudes with frequencies between 0.3 and 3 c/d were detected in the TESS data, which may be high-order γ Dor gravity-mode pulsations. If confirmed, FG Vir would be a hybrid δ Sct/γ Dor variable star.

FG Vir models in the literature were calculated before 2005. FG Vir modelling should be revisited using modern codes in light of new constraints for distance and metallicity, making use of the *K2* and *TESS* data.

Data availability statement

Publicly available datasets were analyzed in this study. These data can be found here: https://mast.stsci.edu/portal/Mashup/Clients/Mast/Portal.html.

Author contributions

JG wrote the text of this article, created the figures and tables, and calculated the FG Vir model discussed. JJ performed the analysis of the FG Vir *Kepler* and *TESS* data, including processing light curves, and performing the pre-whitening analysis to identify significant frequencies and combination frequencies. AH contributed by reviewing literature on possible FG Vir binary companions.

Funding

Acknowledgments

Conflict of interest

The authors declare that the research was conducted in the absence of any commercial or financial relationships that could be construed as a potential conflict of interest.

Publisher's note

References

Abt, H. (1981). Visual multiples. VII. MK classifications. *Astrophys. J. Suppl. Ser.* 45, 437. doi:10.1086/190719

Aerts, C., Christensen-Dalsgaard, J., and Kurtz, D. W. (2010). *Asteroseismology*. New York, New York, United States: Springer Astronomy & Astrophysics Library.

Antoci, V., Cunha, M. S., Bowman, D. M., Murphy, S. J., Kurtz, D. W., Bedding, T. R., et al. (2019). The first view of δ Scuti and γ Doradus stars with the *TESS* mission. *Mon. Not. R. Astron. Soc.* 490, 4040–4059. doi:10.1093/mnras/stz2787

Asplund, M., Amarsi, A. I., and Grevesse, N. (2021). The chemical make-up of the sun: A 2020 vision. *Astron. Astrophys.* 653, A141. doi:10.1051/0004-6361/202140445

Balona, L. A., Daszynska-Daszkiewicz, J., and Pamyatnykh, A. A. (2015). Pulsation frequency distribution in δ Scuti stars. *Mon. Not. R. Astron. Soc.* 452, 3073–3084. doi:10.1093/mnras/stv1513

Balona, L. A. (2014). Low frequencies in Kepler δ Scuti stars. *Mon. Not. R. Astron. Soc.* 437, 1476–1484. doi:10.1093/mnras/stt1981

Baran, A. S., and Koen, C. (2021). A detection threshold in the amplitude spectra calculated from *TESS* time-series data. *Acta Astron.* 71, 113. doi:10.48550/arXiv.2106.09718

Bedding, T., Murphy, S. J., Hey, D. R., Huber, D., Li, T., Smalley, B., et al. (2020). Very regular high-frequency pulsation modes in young intermediate-mass stars. *Nature* 581, 147–151. doi:10.1038/s41586-020-2226-8

Borucki, W. J., Koch, D., Basri, G., Batalha, N., Brown, T., Caldwell, D., et al. (2010). *Kepler* planet-detection mission: Introduction and first results. *Science* 327, 977–980. doi:10.1126/science.1185402

Bowman, D. M., Hermans, J., Daszynska-Daszkiewicz, J., Holdsworth, D. L., Tkachenko, A., Murphy, S. J., et al. (2021). KIC 5950759: A high-amplitude δ Sct star with amplitude and frequency modulation near the terminal age main sequence. *Mon. Not. R. Astron. Soc.* 504, 4039–4053. doi:10.1093/mnras/stab1124

Bowman, D. M., and Kurtz, D. W. (2018). Characterizing the observational properties of δ Sct stars in the era of space photometry from the Kepler mission. *Mon. Notices Royal Astron. Soc.* 476, 3169. doi:10.1093/mnras/sty449

Bowman, D. M., Kurtz, D. W., Breger, M., Murphy, S. J., and Holdsworth, D. L. (2016). Amplitude modulation in δ Sct stars: Statistics from an ensemble study of *Kepler* targets. *Mon. Not. R. Astron. Soc.* 460, 1970–1989. doi:10.1093/mnras/stw1153

Bowman, D. M., and Michielsen, M. (2021). Towards a systematic treatment of observational uncertainties in forward asteroseismic modelling of gravity-mode pulsators. *Astron. Astrophys.* 656, A158. doi:10.1051/0004-6361/202141726

Breger, M., Handler, G., Nather, R. E., Winget, D. E., Kleinman, S. J., Sullivan, D. J., et al. (1995). The δ Scuti star FG Virginis. I. Multiple pulsation frequencies determined with a combined DSN/WET campaign. *A&A* 297, 473.

Breger, M., Handler, G., Serkowitsch, E., Reegen, P., Provencal, J., Wood, M. A., et al. (1996). The δ Scuti star FG Virginis. II. A search for high pulsation frequencies. *A&A* 309, 197.

Breger, M., Lenz, P., Antoci, V., Guggenberger, E., Shobbrook, R. R., Handler, G., et al. (2005). Detection of 75+ pulsation frequencies in the δ Scuti star FG Virginis. *Astron. Astrophys.* 435, 955–965. doi:10.1051/0004-6361:20042480

Breger, M., Lenz, P., and Pamyatnykh, A. A. (2009). Towards mode selection in δ Scuti stars: Regularities in observed and theoretical frequency spectra. *Mon. Not. R. Astron. Soc.* 396, 291–298. doi:10.1111/j.1365-2966.2008.14330.x

Breger, M., and Lenz, P. (2019). Photometric data by the δ Scuti network II. EE cam, FG Vir, 44 tau. *J. Astronomical Data* 25, 1.

Breger, M., and Pamyatnykh, A. A. (2006). Amplitude variability or close frequencies in pulsating stars—The δ Scuti star FG Vir. *Mon. Not. R. Astron. Soc.* 368, 571–578. doi:10.1111/j.1365-2966.2006.10119.x

Breger, M., Pamyatnykh, A. A., Pikall, H., and Garrido, R. (1999). The δ Scuti star FG Vir. IV. Mode identification and pulsation modelling. *A&A* 341, 151.

Breger, M., Rodler, F., Pretorius, M. L., Martin-Ruiz, S., Amado, P. J., Costa, V., et al. (2004). The δ Scuti star FG Vir. V. The 2002 photometric multisite campaign. *Astron. Astrophys.* 419, 695–701. doi:10.1051/0004-6361:20035830

Breger, M., Zima, W., Handler, G., Poretti, E., Shobbrook, R. R., Nitta, A., et al. (1998). The δ Scuti star FG Vir. III. The 1995 multisite campaign and the detection of 24 pulsation frequencies. *A&A* 331, 271.

Brown, A. G. A., Vallenari, A., Prusti, T., de Bruijne, J. H. J., Babusiaux, C., et al. Gaia Collaboration (2021a). Gaia early data release 3. Summary of the contents and survey properties. *A&A* 649, A1. doi:10.48550/arXiv.2012.0153

Brown, A. G. A., Vallenari, A., Prusti, T., de Bruijne, J. H. J., Babusiaux, C., et al. Gaia Collaboration (2021b). Gaia early data release 3. Summary of the contents and survey properties (corrigendum) 2021b. *A&A* 650, C3. doi:10.1051/0004-6361/202039657e

Buchler, J. R., Goupil, M.-J., and Hansen, C. J. (1997). On the role of resonances in nonradial pulsators. *A&A* 321, 159.

Buchler, J. R., and Regev, O. (1983). The effects of nonlinearities on radial and nonradial oscillations. *A&A* 123, 331.

Chevalier, C. (1971). Short-period variables. VIII. Evolution and pulsation of δ-scuti stars. *A&A* 14, 24.

Christensen-Dalsgaard, J. (1993). "Pulsation theory and stellar structure," in Inside the stars, IAU Colloquium 137, ASP Conf. Ser. 40, Austria, April 13–18, 1992.

Cunha, M., Aerts, C., Christensen-Dalsgaard, J., Baglin, A., Bigot, L., Brown, T. M., et al. (2007). Asteroseismology and interferometry. *Astron. Astrophys. Rev.* 14, 217–360. doi:10.1007/s00159-007-0007-0

Daszynska-Daszkiewicz, J., Dziembowski, W. A., Pamyatnykh, A. A., Breger, M., Zima, W., and Houdek, G. (2005). Inferences from pulsational amplitudes and phases for multimodeδSct star FG Vir. *Astron. Astrophys.* 438, 653–660. doi:10.1051/0004-6361:20052902

Daszynska-Daszkiewicz, J., Dziembowski, W. A., and Pamyatnykh, A. A. (2006). On the nature of small amplitude peaks in δ Scuti oscillation spectra. *Mem. S.A.It.* 77, 113.

Daszynska-Daszkiewicz, J., Pamyatnykh, A. A., Walczak, P., Handler, G., Pigulski, A., and Szewczuk, W. (2021). Mode identification and seismic study of δ Scuti, the prototype of a class of pulsating stars. *Mon. Not. R. Astron. Soc.* 505, 88–102. doi:10.1093/mnras/stab1292

Daszynska-Daszkiewicz, J., Walczak, P., Pamyatnykh, A. A., and Szewczuk, W. (2022). Asteroseismology of the double-radial mode δ Scuti star BP Pegasi. *Mon. Not. R. Astron. Soc.* 512, 3551–3565. doi:10.1093/mnras/stac646

Di Criscienzo, M., Ventura, P., D'Antona, F., Marconi, M., Ruoppo, A., and Ripepi, V. (2008). Matching the frequency spectrum of pre-main sequence stars by means of standard and rotating models. *Mon. Not. R. Astron. Soc.* 389, 325–332. doi:10.1111/j.1365-2966.2008.13560.x

Dziembowski, W. (1993). Mode selection and other nonlinear phenomena in stellar oscillations. *Int. Astron. Union Colloq.* 40, 521–534. doi:10.1017/s0252921100018352

Gaia Collaboration (2016). The Gaia mission. *A&A* 595, A1. doi:10.1051/0004-6361/201629272

Gaia Collaboration (2020). VizieR online data catalog: Gaia EDR3, I/350, 2020yCat.1350. *A&A* 649A, 1G. doi:10.5270/esa-1ug

Gilliland, R. L., Brown, T. M., Christensen-Dalsgaard, J., Kjeldsen, H., Aerts, C., Appourchaux, T., et al. (2010). *Kepler* asteroseismology program: Introduction and first results. *PASP* 122, 131–143. doi:10.1086/650399

Goupil, M.-J., and Dziembowski, W. (2000). "Rotational splitting of δ Scuti stars," in ASP Conference Series, Vienna, Austria, 4-7 August.210

Grigahcene, A., Antoci, V., Balona, L., Catanzaro, G., Daszynska-Daszkiewicz, J., Guzik, J. A., et al. (2010). Hybrid γ doradus-δ Scuti pulsators: New insights into the physics of the oscillations from *Kepler* observations. *Astrophys. J.* 713, L192–L197. doi:10.1088/2041-8205/713/2/l192

Guzik, J. A., Garcia, J., and Jackiewicz, J. (2019). Properties of 249 δ Scuti variable star candidates observed during the NASA *K2* mission. *Front. Astron. Space Sci.* 6, 40G. doi:10.3389/fspas.2019.00040

Guzik, J. A., Bradley, P. A., and Templeton, M. R. (2000). "Approaches to asteroseismology of core and shell hydrogen-burning δ Scuti stars," in ASP Conference Series, Vienna, Austria, 4-7 August.210

Guzik, J. A. (2021). Highlights of discoveries for δ Scuti variable stars from the *Kepler* era. *Front. Astron. Space Sci.* 8, 55G. doi:10.3389/fs-pas.2021.653558

Handler, G. (2009). "Delta Scuti variables," in Proceedings of the International Conference "Stellar Pulsation: Challenges for Observation and Theory. Editors J. A. Guzik and P. A. Bradley, 403–409. AIP Conference Proceedings. doi:10.1063/1.32465281170

Howell, S. G., Sobeck, C., Haas, M., Still, M., Barclay, T., Mullally, F., et al. (2014). The *K2* mission: Characterization and early results. *Publ. Astron. Soc. Pac.* 126, 398–408. doi:10.1086/676406

Huber, D., Bryson, S. T., Haas, M. R., Barclay, T., Barentsen, G., Howell, S. B., et al. (2016). The *K2* ecliptic Plane Input catalog (EPIC) and stellar classifications of 138,

600 targets in campaigns 1–8. *Astrophys. J. Suppl. Ser.* 224, 2. doi:10.3847/0067-0049/224/1/2

Kervella, P., Arenou, F., Mignard, F., and Thevenin, F. (2019). Stellar and substellar companions of nearby stars from Gaia DR2: Binarity from proper motion anomaly. *Astron. Astrophys.* 623, 72. doi:10.1051/0004-6361/201834371

Kirbiyik, H., Civelek, R., and Kiziloglu, N. (2004). A new oscillating model suggestion for FG Vir. *Astrophys. Space Sci.* 295, 473–484. doi:10.1007/s10509-005-1085-y

Koch, D. G., Borucki, W. J., Basri, G., Batalha, N. M., Brown, T. M., Caldwell, D., et al. (2010). *Kepler* mission design, realized photometric performance, and early science. *Astrophys. J.* 713, L79–L86. doi:10.1088/2041-8205/713/2/l79

Kurtz, D. W. (2022). "Asteroseismology across the HR diagram," in Annual Reviews of Astronomy and Astrophysics, April 8, 2022.

Kurtz, D. W., Hambleton, K. M., Shibahashi, H., Murphy, S. J., and Prsa, A. (2015). A unifying explanation of complex frequency spectra of γ dor, SPB and Be stars: Combination frequencies and highly non-sinusoidal light curves. *Mon. Not. R. Astron. Soc.* 446, 1223–1233. doi:10.1093/mnras/stu2075

Li, G., Zhao, M., Xie, J., Yao, Y., Mou, L., Zhang, X., et al. (2020). Efficient synthesis of cyclic amidine-based fluorophores *via* 6π-electrocyclic ring closure. *Chem. Sci.* 491, 3586–3591. doi:10.1039/d0sc00798f

Liakos, A., and Niarchos, P. (2017). Catalogue and properties of δ Scuti stars in binaries. *Mon. Not. R. Astron. Soc.* 465, 1181–1200. doi:10.1093/mnras/stw2756

Lopez de Coca, P., Garrido, R., Costa, V., and Rolland, A. (1984). *Narrow band photometry of FG Vir*. Commission 27 of the I.A.U. Budapest, Hungary: International Bulletin on Variable Stars. Number 2465, 27 January.

Mantegazza, L., Poretti, E., and Bossi, M. (1994). Simultaneous intensive photometry and high-resolution spectroscopy of δ Scuti stars. I. Mode typing of HD 106384 = FG Virginis. *A&A* 287, 95.

Mantegazza, L., and Poretti, E. (2002). Line profile variations in the δ Scuti star FG Virginis: A high number of axisymmetric modes. *Astron. Astrophys.* 396, 911–916. doi:10.1051/0004-6361:20021456

Mason, B. D., Wycoff, G. L., Hartkopf, W. I., Douglass, G. G., and Worley, C. E. (2001). The 2001 US naval observatory double star CD-ROM. I. The Washington double star catalog. *Astron. J.* 122, 3466–3471. doi:10.1086/323920

Mighell, K., and Van Cleve, J. (2020). K2*, extending* Kepler's *power to the ecliptic,* K2 *Handbook*. Moffett Field, CA: NASA Ames Research Center. KSCI-19166-003.

Montgomery, M., and O'Donoghue, D. (1999). A derivation of the errors for least squares fitting to time series data. *Delta Scuti Star. Newsl.* 13, 9.

Murphy, S. J., Bedding, T. R., White, T. R., Li李亚光, Y., Hey, D., Reese, D., et al. (2022). Five young δ Scuti stars in the pleiades seen with *Kepler/K2. Mon. Not. R. Astron. Soc.* 511, 5718–5729. doi:10.1093/mnras/stac240

Murphy, S. J., Joyce, M., Bedding, T. R., White, T. R., and Kama, M. (2021). A precise asteroseismic age and metallicity for HD 139614: A pre-main-sequence star with a protoplanetary disc in upper centaurus–lupus. *Mon. Not. R. Astron. Soc.* 502, 1633–1646. doi:10.1093/mnras/stab144

Murphy, S. J., Shibahashi, H., and Kurtz, D. W. (2013). Super-nyquist asteroseismology with the *Kepler* space telescope. *Mon. Not. R. Astron. Soc.* 430, 2986–2998. doi:10.1093/mnras/stt105

Paparo, M., Benko, J. M., Hareter, M., and Guzik, J. A. (2016b). Unexpected series of regular frequency spacing of δ Scuti stars in the non-asymptotic regime. II. Sample-echelle diagrams and rotation. *Astrophys. J. Suppl. Ser.* 224, 41. doi:10.3847/0067-0049/224/2/41

Paparo, M., Benko, J. M., Hareter, M., and Guzik, J. A. (2016a). Unexpected series of regular frequency spacing ofδscuti stars in the non-asymptotic regime. I. The methodology. *Astrophys. J.* 822, 100. doi:10.3847/0004-637x/822/2/100

Papics, P. (2012). The puzzle of combination frequencies found in heat-driven pulsators. *Astron. Nachr.* 333 (10), 1053–1056. doi:10.1002/asna.201211809

Paxton, B., Smolec, R., Schwab, J., Gautschy, A., Bildsten, L., Cantiello, M., et al. (2019). Modules for experiments in stellar Astrophysics (MESA): Pulsating variable stars, rotation, convective boundaries, and energy conservation. *Astrophys. J. Suppl. Ser.* 243, 10. doi:10.3847/1538-4365/ab2241

Poretti, E., Michel, E., Garrido, R., Lefevre, L., Mantegazza, L., Rainer, M., et al. (2009). HD 50844: A new look atδScuti stars from CoRoT space photometry. *Astron. Astrophys.* 506 (1), 85–93. doi:10.1051/0004-6361/200912039

Ricker, G. R., Winn, J. N., Vanderspek, R., Latham, D. W., Bakos, G. A., Bean, J. L., et al. (2015). Transiting exoplanet survey satellite (*TESS*). *J. Astron. Telesc. Instr. Syst.* 1, 014003. doi:10.1117/1.JATIS.1.1.014003

Saio, H. (1981). Rotational and tidal perturbations of nonradial oscillations in a polytropic star. *Astrophys. J.* 244, 299. doi:10.1086/158708

Stassun, K., Oelkers, R. J., Paegert, M., Torres, G., Pepper, J., Lee, N. D., et al. (2019). The revised *TESS* Input catalog and candidate target list. *Astron. J.* 158, 138. doi:10.3847/1538-3881/ab3467

Suarez, J. C., Garcia Hernandez, A., Moya, A., Rodrigo, C., Solano, E., Garrido, R., et al. (2014). Measuring mean densities of Scuti stars with asteroseismology. *Astron. Astrophys.* 563, A7. doi:10.1051/0004-6361/201322270

Templeton, M., Basu, S., and Demarque, P. (2001). Asteroseismology of δ Scuti stars: A parameter study and application to seismology of FG Virginis. *Astrophys. J.* 563, 999–1012. doi:10.1086/324041

Uytterhoeven, K., Moya, A., Grigahcene, A., Guzik, J. A., Gutierrez-Soto, J., Smalley, B., et al. (2011). The *Kepler* characterization of the variability among A- and F-type stars I. General overview. *Astron. Astrophys.* 534, A125. doi:10.1051/0004-6361/201117368

Van Leeuwen, F. (2007). *Hipparcos, the new reduction of the raw DataAstrophysics and space science library*, 350. New York, New York, United States: Springer Science+Business Media B.V. ISBN 978-1-4020-6341-1.

Viskum, M., Kjeldsen, H., Bedding, T. R., and Dall, T. H. (1998). Oscillation mode identifications and models for the δ Scuti star FG Virginis. *A&A* 335, 549.

Zima, W., Wright, D., Bentley, J., Cottrell, P. L., Heiter, U., Mathias, P., et al. (2006). A new method for the spectroscopic identification of stellar non-radial pulsation modes II. Mode identification of the δ Scuti star FG Virginis. *Astron. Astrophys* 455, 235. doi:10.1051/0004-6361:20064877

Zwintz, K., and Steindl, T. (2022). The pre-main sequence: Challenges and prospects for asteroseismology. *Front. Astron. Space Sci.* 9, 914738. doi:10.3389/fspas.2022.914738